Journal of Sound and Vibration (2002) **255**(4), 701–717
doi:10.1006/jsvi.2001.4185, available online at http://www.idealibrary.com on IDEAL®

DYNAMIC CHARACTERISTICS OF STEPPED CANTILEVER BEAMS CONNECTED WITH A RIGID BODY

H.-D. KWON

Center for Information Storage Device, Mechanical Engineering Department, Yonsei University, Seoul 120-749, *South Korea. E-mail: hdkwon@vibcon.yonsei.ac.kr*

AND

Y.-P. PARK

Center for Information Storage Device, Mechanical Engineering Department, Yonsei University, Seoul 120-749, *South Korea*

(*Received* 10 *October* 2000, *and in final form* 22 *July* 2001)

The object of this work is to analyze the dynamic characteristics of the portal frame which consists of two stepped beams including a thin plate and a torsional spring at the discontinuous point and a rigid body connecting each beam tip. This structure is available in a lot of cases that need higher stiffness and linear motion of the tip mass. For example, it might be used for an optical pick-up actuator, using piezoelectric materials, for the high area density CD, DVD or the next generation of optical memory devices, which require superrigidity and linear motion in focusing. The mathematical modelling and the derivation of the equation of motion are given for the cantilevers with identically paralleled and stepped beams. The equation of motion and the associated boundary and the continuous conditions are analytically obtained by using Hamilton's variational principle. The exact solutions are presented and compared with the results obtained by FEM Tool (IDEAS).

1. INTRODUCTION

Over the years, a lot of researches have been done with regard to the vibration of beam structures in many different configurations and complexities. Many studies about the evaluation of the natural frequencies of cantilevered beams with a tip mass exist [1–3]. Rutenburg presents the results of eigenfrequencies of a uniform cantilevered beam with a rotational constraint at some point [4]. Its result indicates that natural frequencies are sensitive to small changes in the location of the rotational spring. Gurgoze and Batan study the eigenfrequencies of a uniform cantilever beam with a rotational and translational constraint at different points [5]. Farghaly considers various constraints at the end boundary in the analysis of the cantilever carrying a tip body [6]. The natural frequency of a stepped beam with two different cross-sections is sought for various boundary conditions by Jang and Bert [7, 8]. Subramanian and Balasubramanian describe the beneficial effects of steps on the dynamic characteristics of beams [9]. They show that it is possible to increase the first natural frequency or to change the natural frequencies by choosing the appropriate thickness ratio and the length ratio of the stepped beam. An exact analytical solution for a cantilever beam of non-uniform cross-section and carrying a mass at the free end has been obtained by Rossi *et al.* [10]. Anderson solves the vibration problem of the

0022-460X/02/$35.00

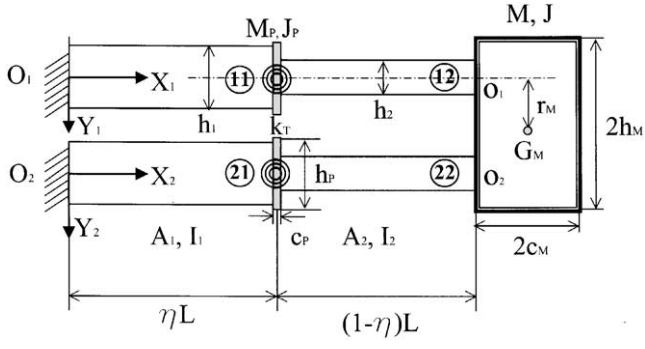

Figure 1. Configuration of two stepped beams with a rigid body at their tip.

two uniform cantilevers joined by a rigid connector at their free ends [11]. He shows the effects of the distance between the two beams and the parameters of the tip connector on the natural frequency of the system. In this paper, we focus on the effect of the position of the stepped point and the thickness ratio on the dynamic characteristics of the system. Also, the evaluation of the natural frequencies of beams with a rotational constraint and a mass located in their intermediate is presented. The beam structure is modelled using the classical beam theory in which the beams comprising this frame are assumed to be uniform and sufficiently slender so that shear deformation and rotary inertia can be ignored. The end conditions raise dynamic coupling between the lateral and longitudinal motion, while the governing equations and continuous conditions do not. We have decided mode styles from the FEM(IDEAS) results which are the bending and the symmetric mode.

2. FORMULATION OF THE PROBLEM

To formulate the equations of motion of this system, we consider the illustration in Figure 1. Let the $O_1X_1Y_1$ and the $O_2X_2Y_2$ axes be inertial frames, and the $o_1x_1y_1$ and the $o_2x_2y_2$ axes be local fixed frames attached to the center of the beam tip. For the present structural system, it is necessary to consider the energies pertaining to the different parts of the system. The first parts of the kinetic energies are due to the lateral and longitudinal motion of the beams, which are expressed by

$$T_s = \frac{1}{2}\int_{\tau_s} \rho(\dot{\mathbf{R}}\cdot\dot{\mathbf{R}})\,\mathrm{d}\tau_s = \frac{1}{2}\int_0^{\eta L} \rho A_1(\dot{u}_{s1}^2 + \dot{v}_{s1}^2)\,\mathrm{d}X_s + \frac{1}{2}\int_{\eta L}^{L} \rho A_2(\dot{u}_{s2}^2 + \dot{v}_{s2}^2)\,\mathrm{d}X_s, \tag{1}$$

where η is a non-dimensional parameter to describe the position of the step. The kinematic variables $u(X,t)$ and $v(X,t)$ represent translational motions in the X and Y directions. Throughout this paper, $s = 1$ and 2 describe the $O_1X_1Y_1$ and $O_2X_2Y_2$ co-ordinates. The right subscripts 1 and 2 of the translations (u and v) denote $0 \leqslant X \leqslant \eta L$ and $\eta L \leqslant X \leqslant L$ respectively. The subscripts to distinguish the beams are given in Figure 1. Considering the illustration in Figure 2, we can define a position vector to describe an arbitrary point of the tip body. An expression of the position vector of the tip body with two vectors can be shown as

$$\begin{aligned}\mathbf{R_M} &= \mathbf{R}(L;t) + \mathbf{r}(x,y) = [L + u_{12}(L;t)]\mathbf{I} + v_{12}(L;t)\mathbf{J} + (c_M + x)\mathbf{i} + (r_M + y)\mathbf{j}\\ &= [L + u_{12}(L;t) + c_M + x - (r_M + y)v'_{12}(L;t)]\mathbf{I}\\ &\quad + [v_{12}(L;t) + (c_M + x)v'_{12}(L;t) + r_M + y]\mathbf{J},\end{aligned} \tag{2}$$

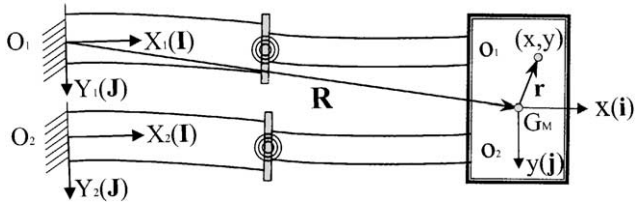

Figure 2. Co-ordinate system and position vector to describe a tip body.

where $\mathbf{i} \approx \mathbf{I} + v'_{12}\mathbf{J}$ and $\mathbf{j} \approx -v'_{12}\mathbf{I} + \mathbf{J}$ for linear system. In these expressions, **I**, **J** and **i**, **j** denote the unit vectors associated with the inertial frame $O_1X_1Y_1$ and the local fixed frame respectively. c_M and h_M designate the distances between the centroid of the tip body and the beam extremity in the x- and y-axis of the local co-ordinate respectively (see Figure 1). The second part of the kinetic energy is due to the laterally and longitudinally coupled motion as well as the lateral, the longitudinal and the rotational motion of the tip body. The kinetic energy of the tip body is given by

$$T_M = \tfrac{1}{2}\int_{\tau M} \rho_M(\dot{\mathbf{R}}_M \cdot \dot{\mathbf{R}}_M)\,\mathrm{d}\tau_M = \tfrac{1}{2}M(\dot{u}_{12}^2 + \dot{v}_{12}^2) + \tfrac{1}{2}J\dot{v}_{12}'^2 + M(c_M\dot{v}_{12}\dot{v}'_{12} - r_M\dot{u}_{12}\dot{v}'_{12}), \quad (3)$$

where $M = 8c_Mh_Mb_M$, $J = (M/3)(c_M^2 + h_M^2) + M(c_M^2 + r_M^2)$.

$2b_M$ is the thickness of the tip body. The tip body is treated as a rigid one with the mass M and moment of the inertia J in the local frame. The kinetic energy of the intermediate plates is

$$T_s^P = \frac{1}{2}\int_0^L \{M_P\dot{v}_{s1}^2 + J_P\dot{v}_{s1}'^2\}\Delta(X_s - \eta_sL)\,\mathrm{d}X_s, \quad (4)$$

where $M_P = c_Ph_Pb_P$, $J_P = (M_P/12)(c_P^2 + h_P^2)$.

Δ denotes the Dirac delta function and b_P is the thickness of the intermediate plate. M_P and J_P are the mass and the moment inertia of the intermediate plate respectively. Two beams have the cross-section area $A = bh$, the second moment of area $I = bh^3/12$, Young's modulus E, the mass density ρ and the length L. The potential energy of the beam due to the bending and extension can be expressed as

$$V_s = \frac{1}{2}\int_{\tau_s} \sigma_{ij}\varepsilon_{ij}\,\mathrm{d}\tau_s = \frac{1}{2}\int_0^{\eta L}(EA_1u_{s1}'^2 + EI_1v_{s1}''^2)\,\mathrm{d}X_s + \frac{1}{2}\int_{\eta L}^{L}(EA_2u_{s2}'^2 + EI_2v_{s2}''^2)\,\mathrm{d}X_s. \quad (5)$$

In this equation, the effects of transverse shear and rotary inertia are ignored. To consider the change of the torsional rigidity at the discontinuous point, i.e, due to some adhesive factor connecting two beams or the extremely high/low ratio of the cross-section area in case that one cross-section cannot include the other cross-section, we assume that the conjunction part at the discontinuous point of the beam is elastically restrained against rotation by a torsional spring. The potential energy of the torsional spring at the point where the spring is attached is written as

$$V_s^T = \frac{1}{2}\int_0^L k_Tv_{s1}'^2\Delta(X_s - \eta_sL)\,\mathrm{d}X_s. \quad (6)$$

3. EQUATIONS OF MOTION

In order to derive the equations of motion of the system that consists of two stepped beams and a rigid connector at their tips, the associated boundary conditions and the continuous conditions at the beam's joints, Hamilton's variational principle is used. It may be stated as

$$\int_{t_1}^{t_2} \delta L \, \mathrm{d}t = \sum_{s=1}^{s=2} \int_{t_1}^{t_2} \left\{ \int_{\tau_s} \sigma_{ij} \delta \varepsilon_{ij} \, \mathrm{d}\tau_s + \delta V_s^T + \rho \int_{\tau_s} \ddot{R} \cdot \delta R \, \mathrm{d}\tau_s - \delta T_M - \delta T_s^P \right\} \mathrm{d}t = 0, \quad (7)$$

where $t = t_1$ and t_2 are two arbitrary instants of time. Substituting the energy described above into Hamilton's principle and integrating by parts, we can obtain the following equations:

$$\begin{aligned}
\delta L = & \sum_{s=1}^{s=2} \int_0^{\eta L} (\rho A_1 \ddot{u}_{s1} - EA_1 u''_{s1}) \delta u_{s1} + (\rho A_1 \ddot{v}_{s1} + EI_1 u'''_{s1}) \delta v_{s1} \, \mathrm{d}X_s \\
& + \int_{\eta L}^{L} (\rho A_2 \ddot{u}_{s2} - EA_2 u''_{s2}) \delta u_{s2} + (\rho A_2 \ddot{v}_{s2} + EI_2 u'''_{s2}) \delta v_{s2} \, \mathrm{d}X_s \\
& - \{ EA_1 u'_{s1} \delta u_{s1} - EI_1 v'''_{s1} \delta v_{s1} + EI_1 v''_{s1} \delta v'_{s1} \}_{X_s = 0} \\
& + \{ EA_1 u'_{s1} \delta u_{s1} - EA_2 u'_{s2} \delta u_{s2} - (EI_1 v'''_{s1} - M_P \ddot{v}_{s1}) \delta v_{s1} + EI_2 v'''_{s2} \delta v_{s2} \\
& \quad + (EI_1 v''_{s1} + k_T v'_{s1} + J_P \ddot{v}'_{s1}) \delta v'_{s1} - EI_2 v''_{s2} \delta v'_{s2} \}_{X_s = \eta L} \\
& + \{ EA_2 u'_{22} \delta u_{22} - EI_2 v'''_{22} \delta v_{22} + EI_2 v''_{22} \delta v'_{22} \\
& \quad + (EA_2 u'_{12} + M\ddot{u}_{12} - Mr_M \ddot{v}'_{12}) \delta u_{12} - (EI_2 v'''_{12} + M\ddot{v}_{12} + Mc_M \ddot{v}'_{12}) \delta v_{12} \\
& \quad + (EI_2 v''_{12} + J\ddot{v}'_{12} + Mc_M \ddot{v}_{12} - Mr_M \ddot{u}_{12}) \delta v'_{12} \}_{X_1 = L} = 0. \qquad (8)
\end{aligned}$$

For very small rotating angle at the end of the beam, we assume that both the two beams have the same deflection and rotating angle, i.e. $v_{12}(L; t) = v_{22}(L; t)$, $v'_{12}(L; t) = v'_{22}(L; t)$, and the relation between the extension and rotating angle, i.e. $u_{12}(L; t) - u_{22}(L; t) = 2r_M v'_{12}(L; t)$. Applying these three constraint boundary conditions to the end boundary conditions of equation (8), we can obtain the following equations:

Governing equations

$$\rho A_1 \ddot{u}_{s1} - EA_1 u''_{s1} = 0, \quad \rho A_1 \ddot{v}_{s1} + EI_1 v''''_{s1} = 0, \qquad 0 \leqslant X_s \leqslant \eta L, \qquad (9a, b)$$

$$\rho A_2 \ddot{u}_{s2} - EA_2 u''_{s2} = 0, \quad \rho A_2 \ddot{v}_{s2} + EI_2 v''''_{s2} = 0, \qquad \eta L \leqslant X_s \leqslant L. \qquad (10a, b)$$

Continuity conditions

At $X_s = \eta L$,

$$u_{s1} - u_{s2} = 0, \quad v_{s1} - v_{s2} = 0, \quad v'_{s1} - v'_{s2} = 0, \quad A_1 u'_{s1} - A_2 u'_{s2} = 0,$$

$$EI_1 v'''_{s1} - M_P \ddot{v}_{s1} - EI_2 v'''_{s2} = 0, \quad EI_1 v''_{s1} + k_T v'_{s1} + J_P \ddot{v}'_{s1} - EI_2 v''_{s2} = 0. \qquad (11a–f)$$

Boundary conditions

At $X_s = 0$,

$$u_{s1} = v_{s1} = v'_{s1} = 0. \tag{12a–c}$$

At $X_s = L$,

$$v_{12} - v_{22} = 0, \quad v'_{12} - v'_{22} = 0, \quad u_{12} - u_{22} - 2r_M v'_{12} = 0,$$

$$EA_2 u'_{12} + EA_2 u'_{22} + M\ddot{u}_{12} - Mr_M \ddot{v}'_{12} = 0,$$

$$EI_2 v''''_{12} + EI_2 v''''_{22} - M\ddot{v}_{12} - Mc_M \ddot{v}'_{12} = 0,$$

$$EI_2 v''_{12} + EI_2 v''_{22} - 2r_M EA_2 u'_{22} + J\ddot{v}'_{12} + Mc_M \ddot{v}_{12} - Mr_M \ddot{u}_{12} = 0. \tag{13a–f}$$

The above 12 boundary conditions and 12 continuity conditions will yield 24 equations in the 24 unknown coefficients.

4. DIMENSIONLESS EXPRESSIONS

$$\eta_s = \frac{X_s}{L}, \quad \bar{u}_{s1} = \frac{u_{s1}}{L}, \quad \bar{v}_{s1} = \frac{v_{s1}}{L}, \quad \bar{u}_{s2} = \frac{u_{s2}}{L}, \quad \bar{v}_{s2} = \frac{v_{s2}}{L}. \tag{14a–e}$$

Dimensionless parameters for the beam

$$\bar{h} = \frac{h_2}{h_1}, \quad \bar{b} = \frac{b_2}{b_1}, \quad \bar{A} = \frac{A_2}{A_1}, \quad \bar{I} = \frac{I_2}{I_1}, \quad \bar{A}^* = \frac{A_2 L^2}{I_1}. \tag{15a–e}$$

Dimensionless parameters for the rigid body

$$\bar{h}_M = \frac{h_M}{L}, \quad \bar{c}_M = \frac{c_M}{L}, \quad \bar{b}_M = \frac{b_M}{L}, \quad \bar{r}_M = \frac{r_M}{L}, \quad \bar{M} = \frac{M}{\rho A_1 L},$$

$$\bar{J}^o = \frac{\bar{M}}{3}(\bar{c}_M^2 + \bar{h}_M^2), \quad \bar{J} = \bar{J}^o + \bar{M}(\bar{c}_M^2 + \bar{r}_M^2). \tag{16a–f}$$

Dimensionless parameters for the intermediate plate and the torsional spring

$$\bar{h}_P = \frac{h_P}{L}, \quad \bar{c}_P = \frac{c_P}{L}, \quad \bar{M}_P = \frac{M_P}{\rho A_1 L}, \quad \bar{J}_P = \frac{\bar{M}_P}{12}(\bar{c}_P^2 + \bar{h}_P^2), \quad \bar{k}_T = \frac{k_T L}{EI_1}. \tag{17a–d}$$

Assumption of solutions. This system executes synchronous motions, defined as motions in which every point performs the same motion in time. Synchronous motions imply that the solution of governing equations can be separated in the space and time. We assume the solutions as follows:

$$\bar{u}_{s1}(\eta_s, t) = \bar{U}_{s1}(\eta_s)e^{i\omega t}, \quad \bar{v}_{s1}(\eta_s, t) = \bar{V}_{s1}(\eta_s)e^{i\omega t}, \qquad 0 \leqslant \eta_s \leqslant \eta, \tag{18a, b}$$

$$\bar{u}_{s2}(\eta_s, t) = \bar{U}_{s2}(\eta_s)e^{i\omega t}, \quad \bar{v}_{s2}(\eta_s, t) = \bar{V}_{s2}(\eta_s)e^{i\omega t}, \qquad \eta \leqslant \eta_s \leqslant 1. \tag{19a, b}$$

Governing equations

$$\bar{U}''_{s1} + \bar{\omega}^2 \bar{U}_{s1} = 0, \quad \bar{V}''''_{s1} - \bar{\lambda}_1^4 \bar{V}_{s1} = 0, \qquad 0 \leqslant \eta_s \leqslant \eta, \tag{20a, b}$$

$$\bar{U}''_{s2} + \bar{\omega}^2 \bar{U}_{s2} = 0, \quad \bar{V}''''_{s2} - \bar{\lambda}_2^4 \bar{V}_{s2} = 0, \qquad \eta \leqslant \eta_s \leqslant 1. \tag{21a, b}$$

Continuity conditions

At $\eta_s = \eta$,

$$\bar{U}_{s1} - \bar{U}_{s2} = 0, \quad \bar{V}_{s1} - \bar{V}_{s2} = 0, \quad \bar{V}'_{s1} - \bar{V}'_{s2} = 0, \quad \bar{U}'_{s1} - \bar{A}\bar{U}'_{s2} = 0,$$

$$\bar{V}'''_{s1} + \bar{\lambda}_1^4 \bar{M}_P \bar{V}_{s1} - \bar{I}\bar{V}'''_{s2} = 0, \qquad \bar{V}''_{s1} + \bar{k}_T \bar{V}'_{s1} - \bar{\lambda}_1^4 \bar{J}_P \bar{V}'_{s1} - \bar{I}\bar{V}''_{s2} = 0. \tag{22a–f}$$

Boundary conditions

At $\eta_s = 0$,

$$\bar{U}_{s1} = \bar{V}_{s1} = \bar{V}'_{s1} = 0. \tag{23a–c}$$

At $\eta_s = 1$,

$$\bar{V}_{12} - \bar{V}_{22} = 0, \quad \bar{V}'_{12} - \bar{V}'_{22} = 0, \quad \bar{U}_{12} - \bar{U}_{22} - 2\bar{r}_M \bar{V}'_{12} = 0,$$

$$\bar{A}\bar{U}'_{12} + \bar{A}\bar{U}'_{22} - \bar{\omega}^2 \bar{M}\bar{U}_{12} + \bar{\omega}^2 \bar{M}\bar{r}_M \bar{V}'_{12} = 0,$$

$$\bar{I}\bar{V}'''_{12} + \bar{I}\bar{V}'''_{22} + \bar{\lambda}_1^4 \bar{M}\bar{V}_{12} + \bar{\lambda}_1^4 \bar{M}\bar{c}_M \bar{V}'_{12} = 0,$$

$$\bar{I}\bar{V}''_{12} + \bar{I}\bar{V}''_{22} - 2\bar{r}_M \bar{A}^* \bar{U}'_{22} - \bar{\lambda}_1^4 \bar{J}\bar{V}'_{12} - \bar{\lambda}_1^4 \bar{M}\bar{c}_M \bar{V}_{12} + \bar{\lambda}_1^4 \bar{M}_M \bar{r}_M \bar{U}_{12} = 0. \tag{24a–f}$$

where

$$\bar{\omega}^2 = \omega^2 \frac{\rho L^2}{E}, \quad \bar{\lambda}_1^4 = \omega^2 \frac{\rho A_1 L^4}{E I_2}, \quad \bar{\lambda}_2^4 = \omega^2 \frac{\rho A_2 L^4}{E I_2}.$$

5. SOLUTION OF THE PROBLEM

The normal mode solutions of the ordinary differential equation are given by

$$\bar{U}_{s1}(\eta_s) = A_{s1} \cos \bar{\omega}\eta_s + B_{s1} \sin \bar{\omega}\eta_s,$$

$$\bar{V}_{s1}(\eta_s) = C_{s1} \cos \bar{\lambda}_1 \eta_s + D_{s1} \sin \bar{\lambda}_1 \eta_s + E_{s1} \cosh \bar{\lambda}_1 \eta_s + F_{s1} \sinh \bar{\lambda}_1 \eta_s, \quad 0 \leqslant \eta_s \leqslant \eta, \tag{25a, b}$$

$$\bar{U}_{s2}(\eta_s) = A_{s2} \cos \bar{\omega}\eta_s + B_{s2} \sin \bar{\omega}\eta_s,$$

$$\bar{V}_{s2}(\eta_s) = C_{s2} \cos \bar{\lambda}_2 \eta_s + D_{s2} \sin \bar{\lambda}_2 \eta_s + E_{s2} \cosh \bar{\lambda}_2 \eta_s + F_{s2} \sinh \bar{\lambda}_2 \eta_s, \quad \eta \leqslant \eta_s \leqslant 1. \tag{26a, b}$$

To determine the natural frequencies and mode shapes for this system, we first substitute equations (25a, b) into the root boundary conditions equations (23a–c), which leads to

$$\text{at } \eta_s = 0, \quad A_{s1} = 0, \quad C_{s1} = -E_{s1}, \quad D_{s1} = -F_{s1}. \tag{27a–c}$$

TABLE 1

Exact solutions and FEM (IDEAS) results for uniform beam ($h_2 = 2$ mm) (unit: Hz)

	ω_1		ω_2		ω_3		ω_4		ω_5	
	Bending mode		Symmetric mode		Bending mode		Bending mode		Symmetric mode	
$h_1/h_2=1$ $k_T=0$	Exact	FEM	Exact	FEM	Exact	FEM	Exact	FEM	Exact	FEM
	409·5	405·2	2550·0	2452·5	2666·1	2609·5	6447·7	6315·5	7029·1	6673·1

TABLE 2

Exact solutions and FEM (IDEAS) results for variation of h_2/h_1 and η ($h_1 = 2$ mm, $k_T = 0$) (unit: Hz)

	$h_2/h_1 = 0{\cdot}2$		$h_2/h_1 = 0{\cdot}4$		$h_2/h_1 = 0{\cdot}5$		$h_2/h_1 = 0{\cdot}6$		$h_2/h_1 = 0{\cdot}8$	
η	Exact	FEM	Exact	FEM	Exact	FEM	Exact	FEM	Exact	FEM
					Bending mode					
First natural frequencies										
0·2	65·5	66·7	169·4	170·2	222·6	222·8	271·9	271·2	352·4	349·6
0·4	100·3	102·2	235·2	234·5	286·3	286·3	323·1	322·5	372·4	370·1
0·5	129·1	132·4	269·7	271·3	309·2	310·0	335·7	335·5	374·0	372·0
0·6	170·1	170·6	294·3	295·9	319·6	320·7	338·2	338·4	373·0	371·1
0·8	258·9	261·6	295·9	297·5	313·0	314·2	332·9	333·0	374·0	372·2
Second natural frequencies										
0·2	805·6	830·0	1523·2	1532·5	1797·9	1798·0	2016·2	2006·4	2358·2	2324·1
0·4	1300·4	1324·4	1698·5	1697·0	1827·7	1833·0	1895·2	1979·0	2339·0	2305·1
0·5	1329·2	1348·1	1557·0	1568·8	1754·2	1757·6	1971·1	1961·1	2370·9	2334·2
0·6	1101·2	1102·4	1532·5	1541·2	1809·0	1808·7	2060·0	2045·3	2432·7	2393·0
0·8	1183·9	1215·7	2012·5	2013·5	2192·1	2186·4	2310·3	2292·6	2495·4	2457·3
Third natural frequencies										
0·2	2158·4	2253·5	3817·9	3847·7	4352·2	4355·0	4806·4	4779·3	5662·3	5569·6
0·4	2370·6	2398·8	3645·0	3624·5	4357·5	4342·7	4975·2	4918·5	5875·0	5763·6
0·5	2325·5	2420·6	4288·0	4312·1	4959·8	4934·4	5421·5	5354·8	6012·2	5899·4
0·6	3261·4	3283·0	5028·3	5013·9	5325·4	5288·9	5564·8	5499·4	6032·1	5917·1
0·8	3969·6	3959·9	4947·5	4919·0	5482·5	5428·2	5871·6	5767·3	6286·3	6152·3
					Symmetric mode					
First natural frequencies										
0·2	788·6	812·8	1475·7	1484·0	1736·7	1734·4	1942·5	1927·0	2260·6	2209·0
0·4	1283·5	1307·8	1665·3	1663·1	1780·7	1780·7	1914·3	1903·9	2233·7	2183·7
0·5	1321·8	1340·9	1520·1	1531·2	1691·1	1692·9	1883·0	1868·9	2253·5	2200·0
0·6	1094·5	1108·0	1470·1	1478·1	1714·4	1712·1	1942·9	1923·6	2301·7	2244·3
0·8	1102·4	1130·1	1843·9	1844·1	2021·7	2013·6	2142·5	2119·2	2342·2	2286·8
Second natural frequencies										
0·2	2164·2	2248·3	3848·0	3879·7	4416·6	4414·3	4920·5	4874·6	5953·6	5771·5
0·4	2373·7	2392·9	3652·0	3628·5	4408·5	4385·8	5099·8	5016·3	6204·8	5989·6
0·5	2336·7	2409·6	4324·9	4349·4	5055·5	5020·7	5583·5	5486·9	6340·5	6128·9
0·6	3265·0	3277·8	5083·5	5013·9	5408·5	5362·6	5695·8	5605·2	6343·7	6129·0
0·8	3971·0	3958·6	4962·0	4929·5	5561·7	5490·7	6041·9	5892·3	6649·9	6394·1

TABLE 3

Exact solutions and FEM (IDEAS) results for variation of h_1/h_2 *and* η ($h_2 = 2\,\text{mm}$, $k_T = 0$) (*unit*: *Hz*)

	$h_1/h_2 = 0{\cdot}2$		$h_1/h_2 = 0{\cdot}4$		$h_1/h_2 = 0{\cdot}5$		$h_1/h_2 = 0{\cdot}6$		$h_1/h_2 = 0{\cdot}8$	
η	Exact	FEM	Exact	FEM	Exact	FEM	Exact	FEM	Exact	FEM
					Bending mode					
First natural frequencies										
0·2	192·7	193·7	245·3	243·1	267·9	265·4	293·9	291·4	352·5	349·4
0·4	118·8	122·1	230·1	229·8	263·3	261·3	291·3	288·5	347·1	343·6
0·5	93·4	96·5	209·7	210·7	252·3	251·6	286·9	285·2	347·3	343·9
0·6	76·3	78·2	186·7	188·0	235·3	235·4	276·8	275·5	345·8	342·7
0·8	56·2	57·3	147·9	149·3	197·0	197·9	245·0	245·0	333·1	331·0
Second natural frequencies										
0·2	1167·1	1187·2	1951·6	1935·9	2142·5	2111·6	2269·4	2228·4	2468·0	2418·5
0·4	1115·5	1093·6	1537·7	1523·3	1793·4	1772·5	2032·9	2004·4	2409·3	2367·1
0·5	1321·8	1248·4	1562·3	1535·8	1752·0	1752·2	1957·7	1930·0	2351·2	2310·3
0·6	1283·5	1271·4	1665·3	1631·4	1806·2	1772·5	1966·8	1930·6	2320·9	2278·8
0·8	796·2	820·4	1485·5	1492·2	1749·3	1740·5	1965·5	1942·4	2325·2	2283·5
Third natural frequencies										
0·2	3668·2	3617·8	4683·2	4647·8	5213·2	5158·7	5618·4	5535·9	6123·6	6010·1
0·4	3195·0	3352·2	4634·5	4600·5	4939·4	4874·1	5230·7	5151·3	5849·2	5748·0
0·5	2252·4	2360·2	4139·5	4172·5	4744·6	4725·8	5172·1	5125·4	5829·9	5732·7
0·6	2015·6	2010·9	3473·7	3490·2	4191·1	4188·2	4809·3	4775·7	5745·1	5658·4
0·8	2108·1	2167·8	3460·1	3428·0	3953·9	3900·8	4448·9	4384·2	5468·1	5380·2
					Symmetric mode					
First natural frequencies										
0·2	1102·3	1110·6	1843·9	1801·8	2021·7	1958·9	2142·6	2067·4	2342·2	2255·4
0·4	1094·5	1047·9	1470·1	1434·5	1714·4	1669·6	1942·9	1886·9	2301·7	2224·0
0·5	1270·5	1265·5	1520·1	1465·0	1691·1	1636·5	1883·0	1826·4	2253·5	2178·2
0·6	1254·7	1304·6	1662·4	1599·0	1777·3	1708·9	1914·3	1844·2	2233·7	2156·2
0·8	788·6	809·5	1475·6	1475·7	1736·7	1713·1	1942·5	1895·5	2260·6	2183·4
Second natural frequencies										
0·2	3969·6	3785·7	4962·0	4812·7	5561·7	5374·6	6041·9	5799·5	6649·9	6336·9
0·4	3261·3	3436·8	5083·5	4931·4	5408·5	5179·7	5695·8	5440·8	6343·7	6053·8
0·5	2325·5	2409·5	4324·9	4314·4	5055·5	4949·5	5583·5	5405·2	6340·5	6053·8
0·6	2370·6	2252·5	3652·0	3605·6	4408·6	4331·4	5099·8	4966·5	6204·8	5954·6
0·8	2158·4	2234·7	3848·0	3769·8	4416·6	4254·4	4920·5	4713·8	5953·5	5692·3

And then substituting more simplified equations (25a, b) and equations (26a, b) into the end boundary and continuity conditions leads to the following set of equations:

$$[a_{m*n}]\{b_n\} = \{0\}, \quad m, n = 1 \sim 18, \tag{28}$$

where $\{b_n\} = \{E_{11}, F_{11}, C_{12}, D_{12}, E_{12}, F_{12}, E_{21}, F_{21}, C_{22}, D_{22}, E_{22}, F_{22}, B_{11}, A_{12}, B_{12}, B_{21}, A_{22}, B_{22}\}^{\mathrm{T}}$.

For the non-trivial solution, the determinant should be zero. The different values of ω and λ_i, which make the value of the determinant to be zero, correspond to the various

natural frequencies of the system. The determinant $|a_{m*n}|$ of this system yields the frequency equation for the system and it is also possible to find the mode shapes $\{b_n\}$ as well. The components of the matrix $[a_{m*n}\}$ are presented in Appendix A.

6. RESULTS AND SUMMARY

To solve this system of equations and to provide a numerical example, the following parameters were used $E = 7{\cdot}5 \times 10^{10}$ Pa, $L = 50 \times 10^{-3}$ m, $\rho = \rho_M = 7800\,\text{kg/m}^3$, $r_M = 4 \times 10^{-3}$ m, $c_M = 5 \times 10^{-3}$ m, $h_M = 5 \times 10^{-3}$ m, $b_M = 5 \times 10^{-3}$ m for Tables 1–3. In

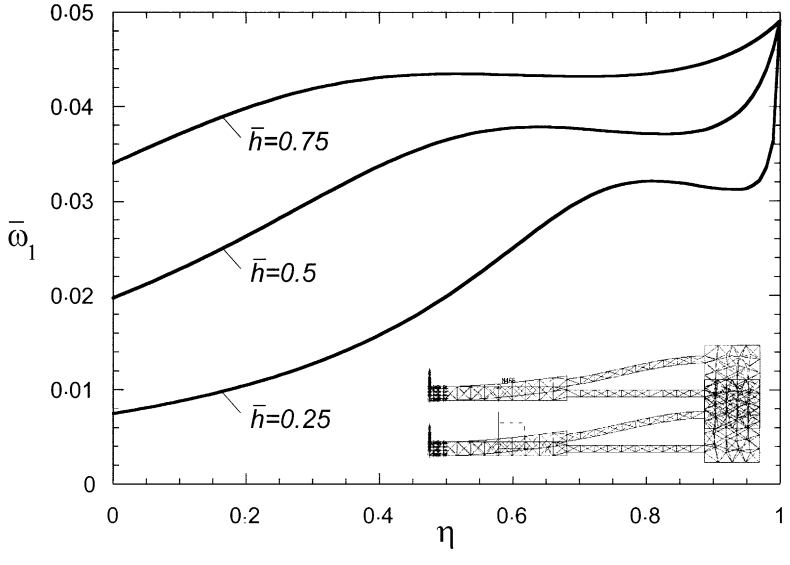

Figure 3. Variation of the fundamental frequency ω_1 versus η for selected values of $\bar{h}$ (bending mode).

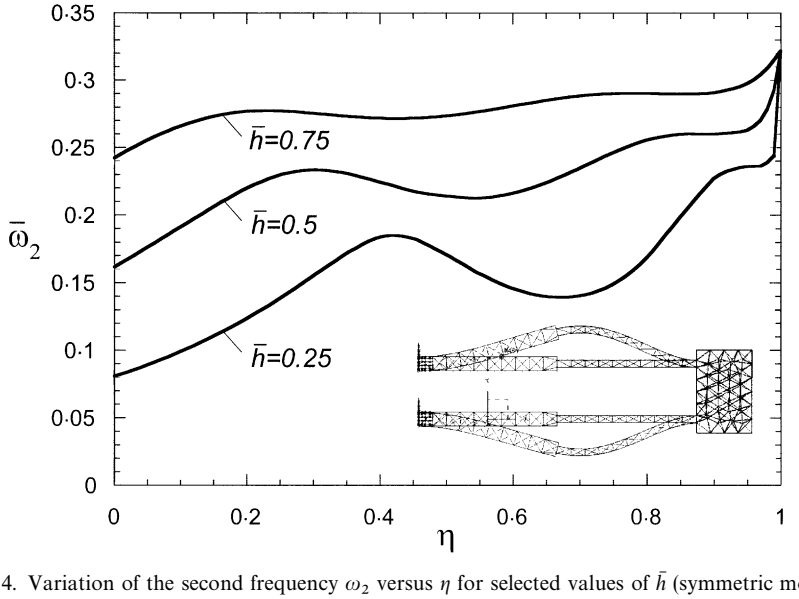

Figure 4. Variation of the second frequency ω_2 versus η for selected values of $\bar{h}$ (symmetric mode).

Table 1, the frequencies of bending modes (ω_1, ω_3 and ω_4) on the exact solutions of closed portal frame with the uniform cross-section are equal to those of Anderson's work [11]. Tables 2 and 3, related with the change of $0 \leqslant h_2/h_1 \leqslant 1$ and $0 \leqslant h_1/h_2 \leqslant 1$, respectively, depict the variation of the three frequencies in bending and two ones in symmetric mode as a function of the thickness ratio for selected values of the stepped points. All frequencies increase with the increase of the thickness ratio.

To find the dynamic characteristics of the non-dimensionalized system, we choose $E = 7{\cdot}5 \times 10^{10}\,\text{Pa}$, $L = 100 \times 10^{-3}\,\text{m}$, $\rho = 7800\,\text{kg/m}^3$, $\bar{\rho}_M = 1$, $h_1 = 5 \times 10^{-3}\,\text{m}$, $b_1 = 10 \times 10^{-3}\,\text{m}$, $\bar{r}_M = 0{\cdot}1$, $c_M = 0{\cdot}1$, $\bar{h}_M = 0{\cdot}15$, $\bar{b}_M = 0{\cdot}05$. Figures 3–5 show the variation

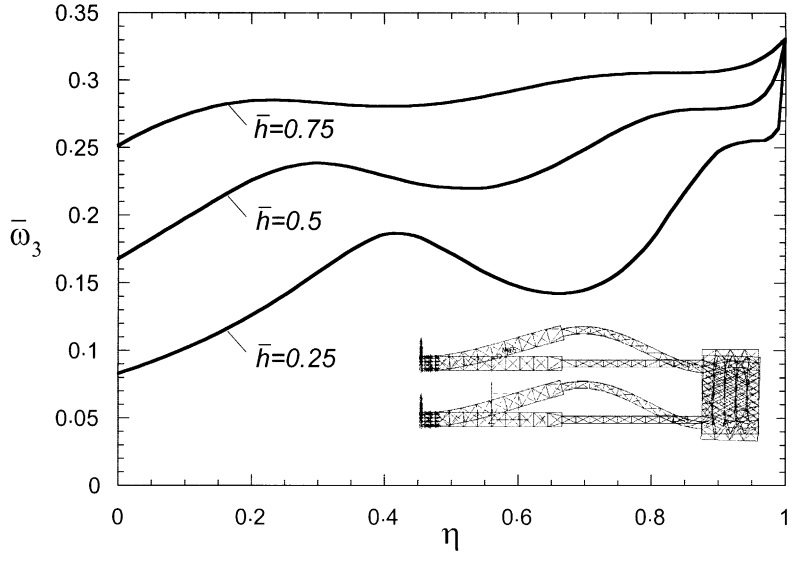

Figure 5. Variation of the third frequency ω_3 versus η for selected values of $\bar{h}$ (bending mode).

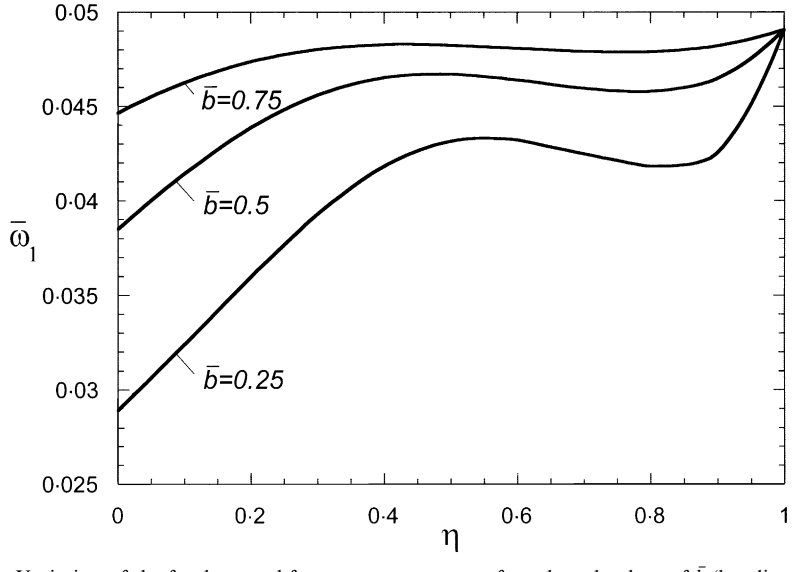

Figure 6. Variation of the fundamental frequency ω_1 versus η for selected values of $\bar{b}$ (bending mode).

of the natural frequency for the stepped position η. The decrease of the step ratio $\bar{h}$ decreases the natural frequency. The natural frequency varies steeply when $\bar{h}$ has small values and the stepped point η is very close to the end of the beam. In Figure 6, the decrease of the step ratio $\bar{b}$ decreases the first natural frequency. However, Figures 7 and 8 show the tendency of the second and third natural frequencies to fall with the increase of $\bar{b}$ for the location of step. In Figure 9, all the natural frequencies go down in correspondence with the decrease of $\bar{h}$. This figure shows that the first mode of this system is clearly different from one of a cantilever beam composed of one beam in which the first natural frequency is larger

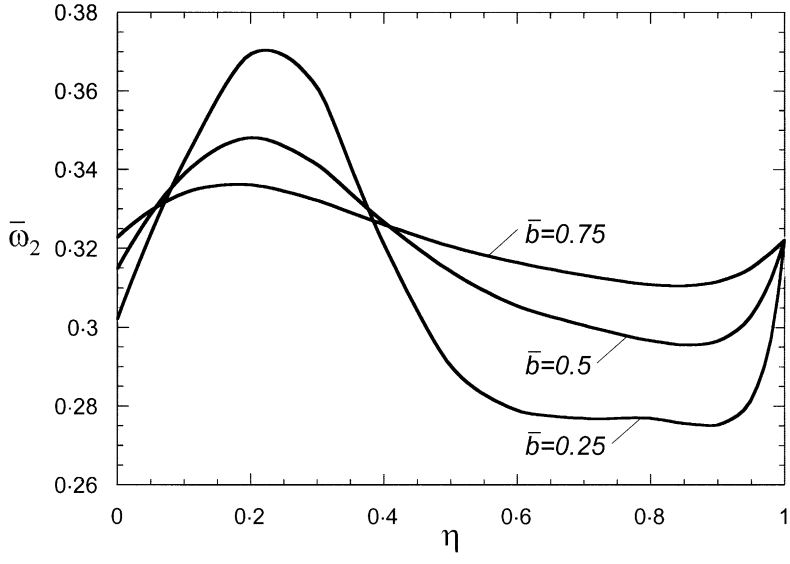

Figure 7. Variation of the second frequency ω_2 versus η for selected values of $\bar{b}$ (symmetric mode).

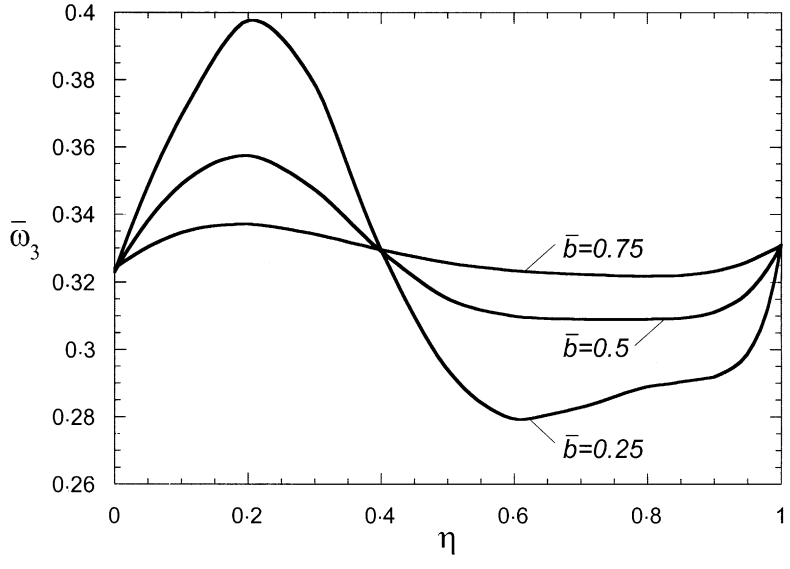

Figure 8. Variation of the third frequency ω_3 versus η for selected values of $\bar{b}$ (bending mode).

than in the uniform beam when step ratios $\bar{h}$ are over 0·3 (see reference [9]). In Figure 10, the natural frequencies except the fifth natural frequency, which is the second natural frequency in symmetric mode, decrease as $\bar{b}$ decreases. For reference, the first and third natural frequencies of the stepped cantilever composed of one beam in bending mode are larger than those of the uniform one when $0{\cdot}1 \leqslant \bar{b} \leqslant 1$ (see reference [9]). In Figures 11–13 for the case of the uniform beam, $\bar{h} = \bar{b} = 1$, the undulating shapes of $\bar{\omega}_1$, $\bar{\omega}_2$ and $\bar{\omega}_3$ are due to the fact that the rotational springs become ineffective when placed at locations with vanishing slopes ($v'_{1s} = 0$, $v'_{2s} = 0$) (see reference [4]). In this system, one can infer that the slopes at the beam tip are very small from the variations of the first and second natural frequencies of the bending mode. The second natural frequency is the symmetric

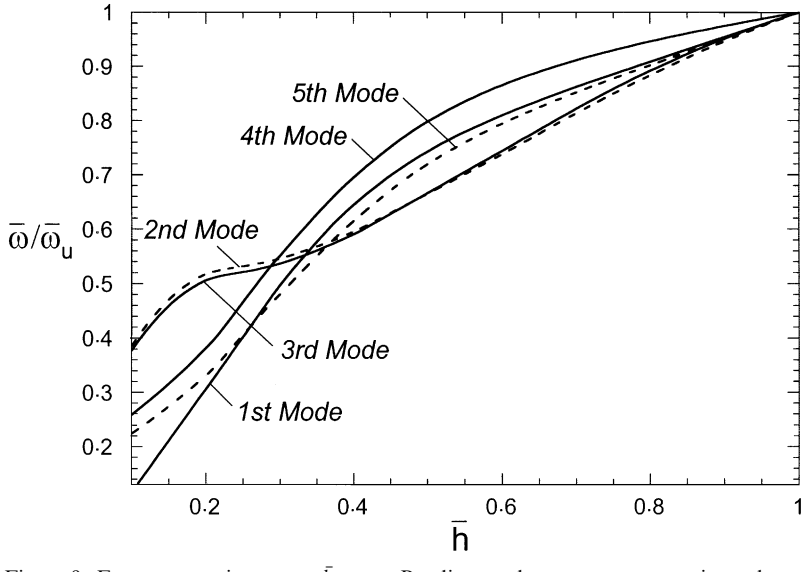

Figure 9. Frequency ratios versus $\bar{h}$. ——: Bending mode; – – – –: symmetric mode.

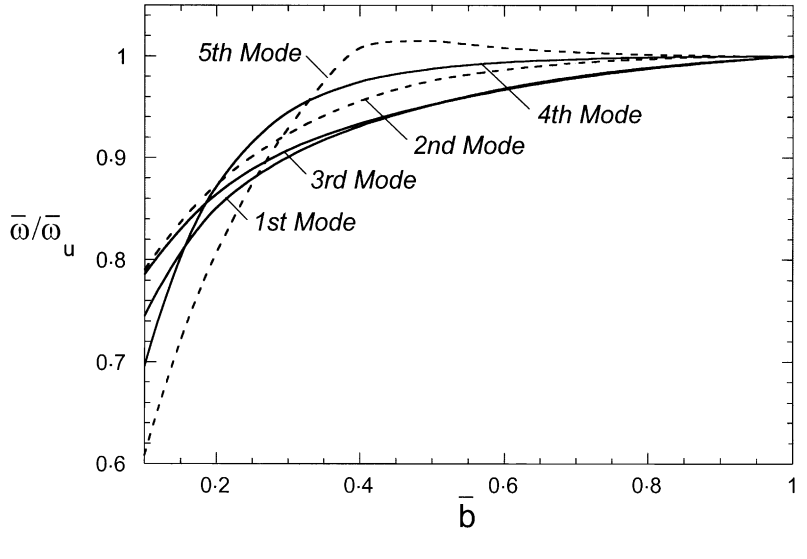

Figure 10. Frequency ratios versus $\bar{b}$. ——: Bending mode; – – – –: symmetric mode.

mode in which the slopes at the end of the beam are vanishing. In Figures 14–16 there are plots depicting the variation of the first three eigenfrequencies for the uniform beam versus η for the non-dimensionalized density of the intermediate plate $\bar{\rho}_P$ when $\bar{h}_P = \bar{b}_P = 0{\cdot}1$ and $\bar{c}_P = 0{\cdot}001$. The fundamental frequencies decrease as $\bar{\rho}_P$ increases. These plots reveal that the variation of $\bar{\rho}_P$ is very effective on the second and third frequencies in the middle of the beam. However, the effectiveness of $\bar{\rho}_P$ vanishes at both boundaries.

The exact expressions for eigenfrequencies have been presented on the rotationally constrained and stepped portal frame with intermediate mass. The reliability of the results

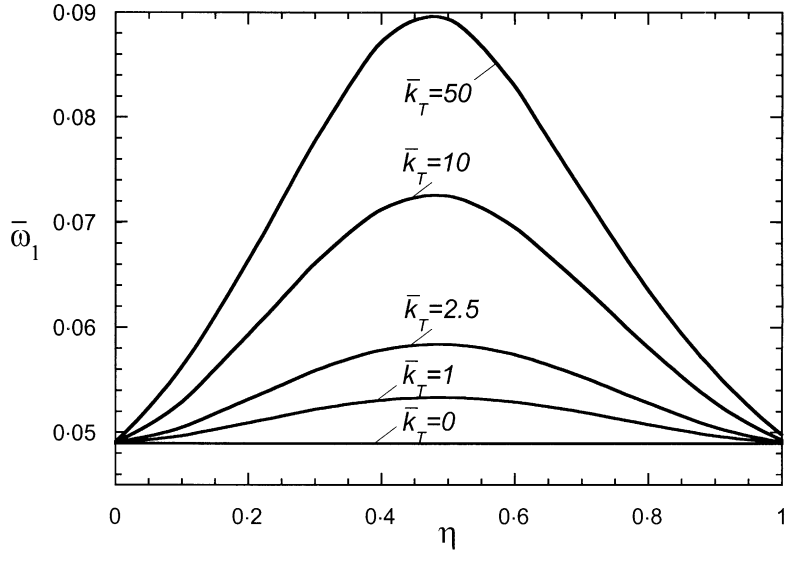

Figure 11. Variation of the fundamental frequency ω_1 versus η for selected values of $\bar{k}_T$ (bending mode).

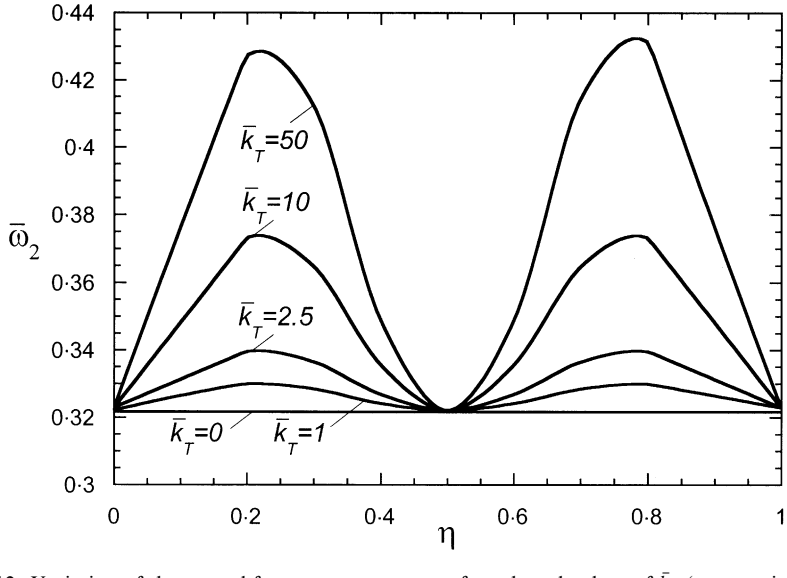

Figure 12. Variation of the second frequency ω_2 versus η for selected values of $\bar{k}_T$ (symmetric mode).

for the present study has been verified by comparing the results from FEM method (commercial software IDEAS). Adjusting the thickness ratio and the length ratio of the stepped beams, we can obtain the beneficial effects of frequency tuning to achieve a desired dynamic behavior without altering considerably the frequencies of the other modes as well as we can do structural tailoring to avoid resonance in various situations. We can modify the dynamic characteristics of the system by considering the torsional spring at the beam joint. In this paper, we present the variation of frequency according to the value of the torsional spring.

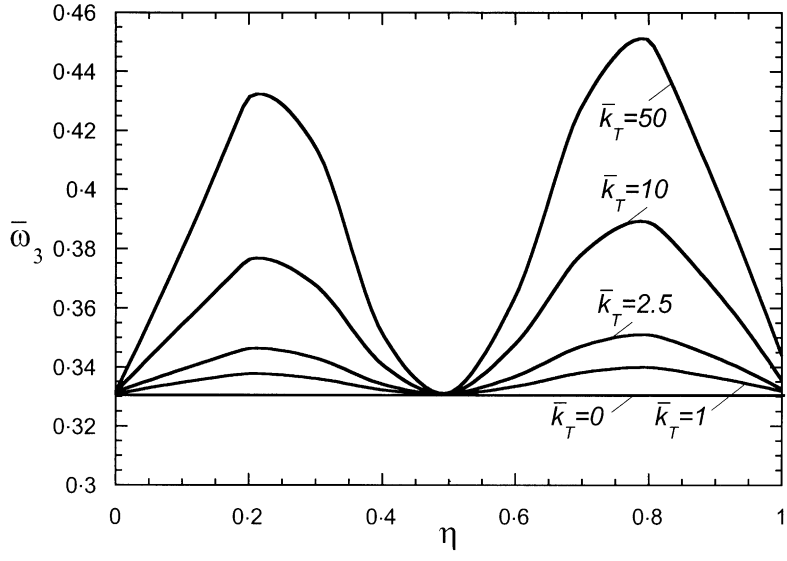

Figure 13. Variation of the third frequency ω_3 versus η for selected values of $\bar{k}_T$ (bending mode).

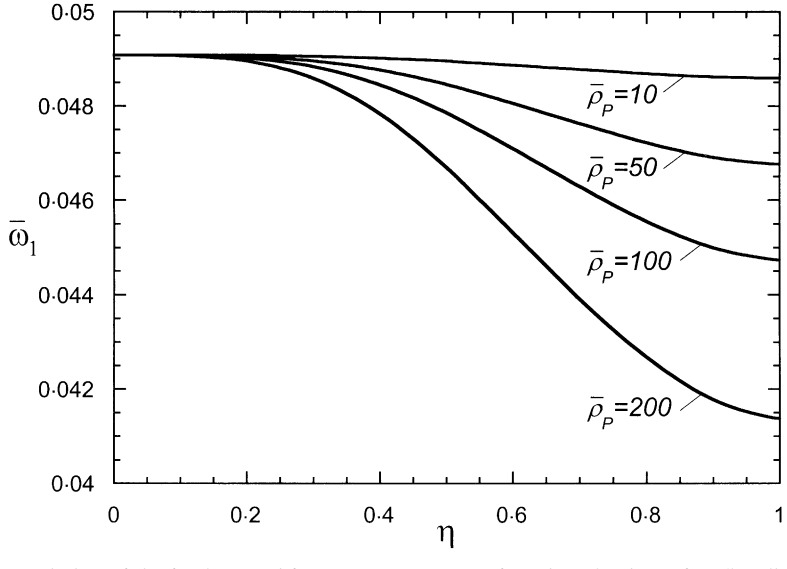

Figure 14. Variation of the fundamental frequency ω_1 versus η for selected values of $\bar{\rho}_P$ (bending mode).

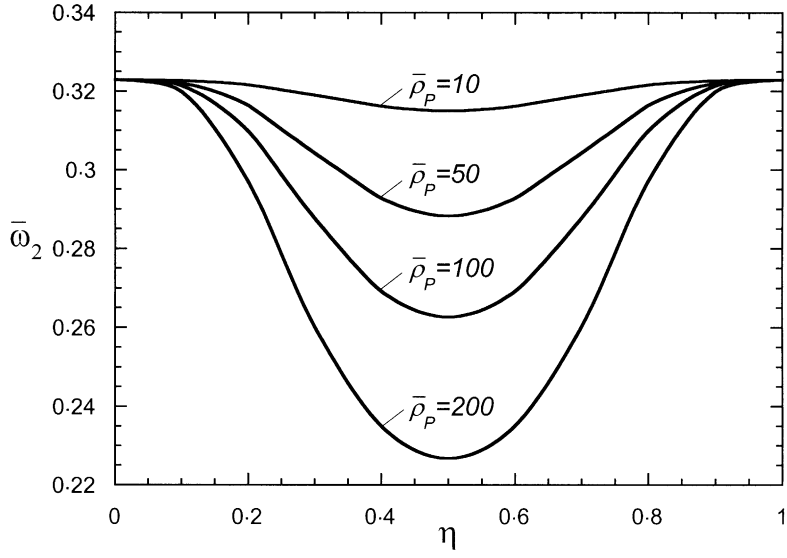

Figure 15. Variation of the second frequency ω_2 versus η for selected values of $\bar{\rho}_P$ (bending mode).

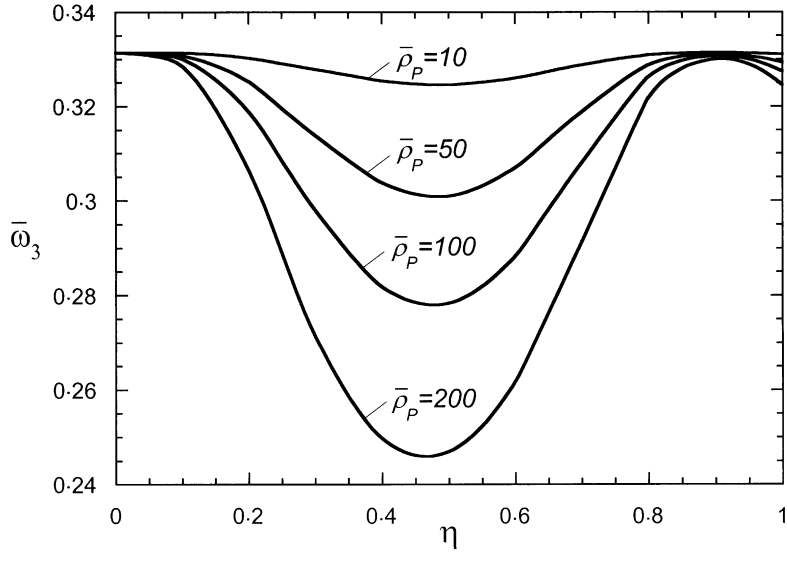

Figure 16. Variation of the third frequency ω_3 versus η for selected values of $\bar{\rho}_P$ (bending mode).

ACKNOWLEDGMENTS

This work was funded by the Korea Science and Engineering Foundation (KOSEF) through the Center for Information Storage Device (CISD) Grant No. 2001G0101.

REFERENCES

1. P. A. A. Laura, J. L. Pombo and E. A. Susemihl 1974 *Journal of Sound and Vibration* **37**, 161–168. A note on the vibrations of a clamped-free beam with a mass at the free end.

2. B. RAMA BHAT and H. WAGNER 1976 *Journal of Sound and Vibration* **44**, 304–307. Natural frequencies of a uniform cantilever with a tip mass slender in the axial direction.
3. B. RAMA BHAT and M. AVINASH KULKARNI 1976 *American Institute of Aeronautics and Astronautics* **14**, 536–537. Natural frequencies of a cantilever with slender tip mass.
4. A. RUTENBERG 1978 *American Society of Mechanical Engineers Journal of Applied Mechanics* **45**, 422–423. Vibration frequencies for a uniform cantilever with a rotational constraint at a point.
5. M. GURGOZE and H. BATAN 1986 *Journal of Sound and Vibration* **106**, 533–536. A note on the vibrations of a restrained cantilever beam carrying a heavy tip body.
6. S. H. FARGHALY 1992 *Journal of Sound and Vibration* **156**, 323–380. Bending vibration of an axially loaded cantilever beam with an elastically mounted end mass of finite length.
7. S. K. JANG and C. W. BERT 1989 *Journal Sound and Vibration* **130**, 342–346. Free vibration of stepped beams: exact and numerical solutions.
8. S. K. JANG and C. W. BERT 1989 *Journal of Sound and Vibration* **132**, 164–168. Free vibration of stepped beams: higher mode frequencies and effects of steps on frequency.
9. G. SUBRAMANIAN and T. S. BALASUBRAMANIAN 1987 *Journal of Sound and Vibration* **118**, 555–560. Beneficial effects of steps on the free vibration characteristics of beams.
10. R. E. ROSSI, P. A. A. LAURA and R. H. GUTIERREZ 1990 *Journal of Sound and Vibration* **143**, 491–502. A note on transverse vibrations of a Timoshenko beam of non-uniform thickness clamped at one end and carrying a concentrated mass at the other.
11. G. L. ANDERSON 1978 *Journal of Sound and Vibration* **57**, 403–412. Natural frequencies of two cantilevers joined by rigid connector at their free ends.
12. L. MEIROVITCH 1967 *Analytical Methods in Vibrations*. New York: Macmillan.

APPENDIX A: COMPONENTS OF THE MATRIX $[a_{m*n}]$

$$a_{1*1} = a_{11*7} = -\cos\bar{\lambda}_1\eta + \cosh\bar{\lambda}_1\eta, \quad a_{1*2} = a_{11*8} = -\sin\bar{\lambda}_1\eta + \sinh\bar{\lambda}_1\eta,$$

$$a_{1*3} = a_{11*9} = -\cos\bar{\lambda}_2\eta, \quad a_{1*4} = a_{11*10} = -\sin\bar{\lambda}_2\eta, \quad a_{1*5} = a_{11*11} = -\cosh\bar{\lambda}_2\eta,$$

$$a_{1*6} = a_{11*12} = -\sinh\bar{\lambda}_2\eta,$$

$$a_{2*1} = a_{12*7} = -\bar{\lambda}_1^3(\sin\bar{\lambda}_1\eta - \sinh\bar{\lambda}_1\eta) - \bar{\lambda}_1^4 M_P(\cos\bar{\lambda}_1\eta - \cosh\bar{\lambda}_1\eta),$$

$$a_{2*2} = a_{12*8} = \bar{\lambda}_1^3(\cos\bar{\lambda}_1\eta + \cosh\bar{\lambda}_1\eta) - \bar{\lambda}_1^4\bar{M}_P(\sin\bar{\lambda}_1\eta - \sinh\bar{\lambda}_1\eta),$$

$$a_{2*3} = a_{12*9} = -\bar{I}\bar{\lambda}_2^3\sin\bar{\lambda}_2\eta, \quad a_{2*4} = a_{12*10} = \bar{I}\bar{\lambda}_2^3\cos\bar{\lambda}_2\eta,$$

$$a_{2*5} = a_{12*11} = -\bar{I}\bar{\lambda}_2^3\sinh\bar{\lambda}_2\eta, \quad a_{2*6} = a_{12*12} = -\bar{I}\bar{\lambda}_2^3\cosh\bar{\lambda}_2\eta,$$

$$a_{3*1} = a_{13*7} = \bar{\lambda}_1(\sin\bar{\lambda}_1\eta + \sinh\bar{\lambda}_1\eta), \quad a_{3*2} = a_{13*8} = -\bar{\lambda}_1(\cos\bar{\lambda}_1\eta - \cosh\bar{\lambda}_1\eta),$$

$$a_{3*3} = a_{13*9} = \bar{\lambda}_2\sin\bar{\lambda}_2\eta, \quad a_{3*4} = a_{13*10} = -\bar{\lambda}_2\cos\bar{\lambda}_2\eta,$$

$$a_{3*5} = a_{13*11} = -\bar{\lambda}_2\sinh\bar{\lambda}_2\eta, \quad a_{3*6} = a_{13*12} = -\bar{\lambda}_2\cosh\bar{\lambda}_2\eta,$$

$$a_{4*1} = a_{14*7} = \bar{\lambda}_1^2(\cos\bar{\lambda}_1\eta + \cosh\bar{\lambda}_1\eta) + (\bar{k}_T - \bar{\lambda}_1^4\bar{J}_P)\bar{\lambda}_1(\sin\bar{\lambda}_1\eta + \sinh\bar{\lambda}_1\eta),$$

$$a_{4*2} = a_{14*8} = \bar{\lambda}_1^2(\sin\bar{\lambda}_1\eta + \sinh\bar{\lambda}_1\eta) + (\bar{k}_T - \bar{\lambda}_1^4\bar{J}_P)\bar{\lambda}_1(-\cos\bar{\lambda}_1\eta + \cosh\bar{\lambda}_1\eta),$$

$$a_{4*3} = a_{14*9} = \bar{I}\bar{\lambda}_2^2\cos\bar{\lambda}_2\eta, \quad a_{4*4} = a_{14*10} = \bar{I}\bar{\lambda}_2^2\sin\bar{\lambda}_2\eta,$$

$$a_{4*5} = a_{14*11} = -\bar{I}\bar{\lambda}_2^2\cosh\bar{\lambda}_2\eta, \quad a_{4*6} = a_{14*12} = -\bar{I}\bar{\lambda}_2^2\sinh\bar{\lambda}_2\eta,$$

$$a_{5*3} = -\bar{I}\bar{\lambda}_2^3 \sin\bar{\lambda}_2 - \bar{\lambda}_1^4\bar{M}(\cos\bar{\lambda}_2 - \bar{\lambda}_2\bar{c}_M \sin\bar{\lambda}_2),$$

$$a_{5*4} = \bar{I}\bar{\lambda}_2^3 \cos\bar{\lambda}_2 - \bar{\lambda}_1^4\bar{M}(\sin\bar{\lambda}_2 - \bar{\lambda}_2\bar{c}_M \cos\bar{\lambda}_2),$$

$$a_{5*5} = -\bar{I}\bar{\lambda}_2^3 \sinh\bar{\lambda}_2 - \bar{\lambda}_1^4\bar{M}(\cosh\bar{\lambda}_2 + \bar{\lambda}_2\bar{c}_M \sinh\bar{\lambda}_2),$$

$$a_{5*6} = -\bar{I}\bar{\lambda}_2^3 \cos\bar{\lambda}_2 - \bar{\lambda}_1^4\bar{M}(\sinh\bar{\lambda}_2 + \bar{\lambda}_2\bar{c}_M \cosh\bar{\lambda}_2),$$

$$a_{5*9} = -\bar{I}\bar{\lambda}_2^3 \sin\bar{\lambda}_2,\ a_{5*10} = \bar{I}\bar{\lambda}_2^3 \cos\bar{\lambda}_2,\ a_{5*11} = -\bar{I}\bar{\lambda}_2^3 \sinh\bar{\lambda}_2,\ a_{5*12} = -\bar{I}\bar{\lambda}_2^3 \cosh\bar{\lambda}_2,$$

$$a_{6*3} = -\bar{I}\bar{\lambda}_2^2 \cos\bar{\lambda}_2 - \bar{\lambda}_1^4(\bar{M}\bar{c}_M \cos\bar{\lambda}_2 - \bar{J}\bar{\lambda}_2 \sin\bar{\lambda}_2),$$

$$a_{6*4} = -\bar{I}\bar{\lambda}_2^2 \sin\bar{\lambda}_2 - \bar{\lambda}_1^4(\bar{M}\bar{c}_M \sin\bar{\lambda}_2 + \bar{J}\bar{\lambda}_2 \cos\bar{\lambda}_2),$$

$$a_{6*5} = \bar{I}\bar{\lambda}_2^2 \cosh\bar{\lambda}_2 - \bar{\lambda}_1^4(\bar{M}\bar{c}_M \cosh\bar{\lambda}_2 + \bar{J}\bar{\lambda}_2 \sinh\bar{\lambda}_2),$$

$$a_{6*6} = \bar{I}\bar{\lambda}_2^2 \sinh\bar{\lambda}_2 - \bar{\lambda}_1^4(\bar{M}\bar{c}_M \sinh\bar{\lambda}_2 + \bar{J}\bar{\lambda}_2 \cosh\bar{\lambda}_2),$$

$$a_{6*9} = -\bar{I}\bar{\lambda}_2^2 \cos\bar{\lambda}_2,\quad a_{6*10} = -\bar{I}\bar{\lambda}_2^2 \sin\bar{\lambda}_2,\quad a_{6*11} = \bar{I}\bar{\lambda}_2^2 \cosh\bar{\lambda}_2,\quad a_{6*12} = \bar{I}\bar{\lambda}_2^2 \sinh\bar{\lambda}_2,$$

$$a_{6*14} = \bar{\lambda}_1^4\bar{M}\bar{r}_M \cos\bar{\omega},\quad a_{6*15} = \bar{\lambda}_1^4\bar{M}\bar{r}_M \sin\bar{\omega},\quad a_{6*17} = 2\bar{r}_M\bar{A}^*\bar{\omega}\sin\bar{\omega},$$

$$a_{6*18} = -2\bar{r}_M\bar{A}^*\bar{\omega}\cos\bar{\omega},$$

$$a_{7*3} = 2\bar{r}_M\bar{\lambda}_2 \sin\bar{\lambda}_2,\quad a_{7*4} = -2\bar{r}_M\bar{\lambda}_2 \cos\bar{\lambda}_2,\quad a_{7*5} = -2\bar{r}_M\bar{\lambda}_2 \sinh\bar{\lambda}_2,$$

$$a_{7*6} = -2\bar{r}_M\bar{\lambda}_2 \cosh\bar{\lambda}_2,$$

$$a_{7*14} = -a_{7*17} = \cos\bar{\omega},\quad a_{7*15} = -a_{7*18} = \sin\bar{\omega},$$

$$a_{8*3} = -\bar{\omega}^2\bar{M}\bar{r}_M\bar{\lambda}_2 \sin\bar{\lambda}_2,\quad a_{8*4} = \bar{\omega}^2\bar{M}\bar{r}_M\bar{\lambda}_2 \cos\bar{\lambda}_2,\quad a_{8*5} = \bar{\omega}^2\bar{M}\bar{r}_M\bar{\lambda}_2 \sinh\bar{\lambda}_2,$$

$$a_{8*6} = \bar{\omega}^2\bar{M}\bar{r}_M\bar{\lambda}_2 \cosh\bar{\lambda}_2,\quad a_{8*14} = -\bar{A}\bar{\omega}\sin\bar{\omega} - \bar{\omega}^2\bar{M}\cos\bar{\omega},$$

$$a_{8*15} = \bar{A}\bar{\omega}\cos\bar{\omega} - \bar{\omega}^2\bar{M}\sin\bar{\omega},\quad a_{8*17} = -\bar{A}\bar{\omega}\sin\bar{\omega},\quad a_{8*18} = \bar{A}\bar{\omega}\cos\bar{\omega},$$

$$a_{9*3} = -a_{9*9} = \cos\bar{\lambda}_2,\quad a_{9*4} = -a_{9*10} = \sin\bar{\lambda}_2,$$

$$a_{9*5} = -a_{9*11} = \cosh\bar{\lambda}_2,\quad a_{9*6} = -a_{9*12} = \sinh\bar{\lambda}_2,$$

$$a_{10*3} = -a_{10*9} = -\bar{\lambda}_2 \sin\bar{\lambda}_2,\quad a_{10*4} = -a_{10*10} = \bar{\lambda}_2 \cos\bar{\lambda}_2,$$

$$a_{10*5} = -a_{10*11} = \bar{\lambda}_2 \sinh\bar{\lambda}_2,\quad a_{10*6} = -a_{10*12} = \bar{\lambda}_2 \cosh\bar{\lambda}_2,$$

$$a_{15*13} = a_{17*16} = \sin\bar{\omega}\eta,\quad a_{15*14} = a_{17*17} = -\cos\bar{\omega}\eta,$$

$$a_{15*15} = a_{17*18} = -\sin\bar{\omega}\eta,$$

$$a_{16*13} = a_{18*16} = \bar{\omega}\cos\bar{\omega}\eta,\quad a_{16*14} = a_{18*17} = \bar{A}\bar{\omega}\sin\bar{\omega}\eta,$$

$$a_{16*15} = a_{18*18} = -\bar{A}\bar{\omega}\cos\bar{\omega}\eta.$$